Microfluidic experiments reveal that antifreeze proteins bound to ice crystals suffice to prevent their growth

Yeliz Celik[a], Ran Drori[b], Natalya Pertaya-Braun[a], Aysun Altan[a], Tyler Barton[a], Maya Bar-Dolev[b], Alex Groisman[c], Peter L. Davies[d], and Ido Braslavsky[a,b,1]

[a]Department of Physics and Astronomy, Ohio University, Athens, OH 45701; [b]Institute of Biochemistry, Food Science, and Nutrition, Robert H. Smith Faculty of Agriculture, Food, and Environment, The Hebrew University of Jerusalem, Rehovot 76100, Israel; [c]Department of Physics, University of California at San Diego, La Jolla, CA 92093; and [d]Department of Biomedical and Molecular Sciences, Queen's University, Kingston, ON, Canada K7L 3N6

Edited by David A. Weitz, Harvard University, Cambridge, MA, and approved December 12, 2012 (received for review August 22, 2012)

Antifreeze proteins (AFPs) are a subset of ice-binding proteins that control ice crystal growth. They have potential for the cryopreservation of cells, tissues, and organs, as well as for production and storage of food and protection of crops from frost. However, the detailed mechanism of action of AFPs is still unclear. Specifically, there is controversy regarding reversibility of binding of AFPs to crystal surfaces. The experimentally observed dependence of activity of AFPs on their concentration in solution appears to indicate that the binding is reversible. Here, by a series of experiments in temperature-controlled microfluidic devices, where the medium surrounding ice crystals can be exchanged, we show that the binding of hyperactive *Tenebrio molitor* AFP to ice crystals is practically irreversible and that surface-bound AFPs are sufficient to inhibit ice crystal growth even in solutions depleted of AFPs. These findings rule out theories of AFP activity relying on the presence of unbound protein molecules.

thermal hysteresis | ice structuring proteins

Antifreeze proteins (AFPs) are found in a variety of cold-adapted organisms, where they serve as inhibitors of ice crystal growth and recrystallization (1, 2). These proteins are a subset of an expanding group of identified proteins, whose salient feature is ice binding (3, 4). AFPs are characterized by their ability to cause a temperature difference (hysteresis) in the melting and freezing of ice and are classified as hyperactive or moderately active according to the magnitude of their freezing hysteresis (FH) activity (5). The FH activity is defined as the difference between the melting temperature of ice crystals and the nonequilibrium freezing temperature at which rapid crystal growth commences. Although the FH activity has been investigated for more than four decades, the actual mechanism of action of AFPs is still not clear. This is partly because the interactions between molecules of AFPs, water, and ice at the ice–water interface are difficult to study experimentally due to the delicate, transitory nature of the ice–water interface.

FH activity is thought to be due to an adsorption-inhibition mechanism that states that AFPs bind to ice surfaces and allow ice crystal growth only in surface regions between the bound AFP molecules (6, 7). This patchy growth pattern causes increased local microcurvature of the ice front that leads to larger surface energy, making the transformation of water into ice less energetically favorable and thus reducing the freezing temperature (Gibbs–Thompson effect). It has been argued that the binding of AFPs to ice surfaces must be irreversible, because AFP desorption would result in rapid crystal growth in the areas where the AFP molecules have been desorbed from the ice surface (6, 8). This theory has been criticized for assuming that the ice–water interface is sharp, contrary to the experimental evidence that the transitions from an ordered solid phase to a liquid phase at the ice–water interfaces are gradual and occur over several layers of water molecules (9–12). Perhaps the hardest criticism to answer is related to the experimentally observed dependence of FH activity on AFP concentration, which strongly suggests a dynamic exchange between adsorbed AFPs and free AFPs in the surrounding solution (11, 13–18).

A few theories relating the kinetics of adsorption of AFP molecules to the ice surface with the observed FH activity have been suggested (19, 20). Several experimental studies have examined the kinetics of AFP binding to ice, but the questions of reversibility of the AFP binding and of the contribution of AFP molecules in solution to the inhibition of ice growth have not been resolved. For instance, Ba et al. used NMR to study the binding of fish type I AFPs to ice and suggested that an increment in the NMR signal over time was an evidence of desorption of AFP molecules from the ice surface (21). Additionally, based on the observed loss of fluorescence intensity at an edge of a growing ice crystal in experiments with fluorescently labeled antifreeze glycoproteins, Zepeda et al. argued that AFPs on the ice surface were released upon growth of a new layer of ice (9). Thus, the authors concluded that the binding of these proteins to the ice surface was weak. In contrast to the above results, Pertaya et al. (22), who used fish AFP type III (23) tagged with green fluorescent protein (GFP) and the technique of fluorescence recovery after photobleaching (FRAP), found the binding of AFPs to ice surfaces to be irreversible. Nevertheless, these experiments did not directly address the question of the influence of AFPs in solution on the FH activity. To answer this question, one needs to be able to vary the concentration of AFPs in solution in the vicinity of ice crystals without perturbing the crystals or changing the amount of AFPs bound to their surfaces.

Recently, microfluidic devices have been used to study ice nucleation processes (24–26), cell injury by freezing (27), and thaw–freezing cycle valves (28). Here we used a sensitive temperature-controlled system and custom-built microfluidic devices to slowly remove AFPs from the solution around individual ice crystals without perturbing the crystals or changing the temperature. The AFPs were fused with GFP, enabling their visualization in solution and on ice crystals under a fluorescence microscope. Our experiments provide direct evidence that the binding of hyperactive *Tenebrio molitor* AFP (*Tm*AFP) molecules to ice crystals is practically irreversible and that, at a given amount of AFPs bound to an ice crystal surface, the FH activity is virtually independent of the concentration of AFPs in solution. These findings contradict a broadly accepted view that the FH activity depends on the

Author contributions: Y.C., N.P.-B., P.L.D., and I.B. designed research; Y.C., R.D., A.A., and I.B. performed research; T.B., M.B.-D., and A.G. contributed new reagents/analytic tools; Y.C., R.D., and I.B. analyzed data; and Y.C., M.B.-D., A.G., P.L.D., and I.B. wrote the paper.

The authors declare no conflict of interest.

This article is a PNAS Direct Submission.

Freely available online through the PNAS open access option.

[1]To whom correspondence should be addressed. E-mail: braslavs@agri.huji.ac.il.

This article contains supporting information online at www.pnas.org/lookup/suppl/doi:10.1073/pnas.1213603110/-/DCSupplemental.

concentration of AFPs in solution, suggesting that the existing theories relating the concentration of AFPs in solution to the observed FH activity need to be reexamined.

Results

Exchanging GFP-AFP Solution Around an Ice Crystal. The reversibility of binding of AFPs to ice was examined in a solution-exchange experiment. The microfluidic devices used in the experiments were designed to allow the growth of an ice crystal in a small chamber, with an option to exchange the solution around the ice crystal at minimal flow rate, thus minimizing the perturbation to the crystal (Figs. 1 and 2*A* and *Materials and Methods*). The protein used in the study was a fusion of the insect hyperactive *Tm*AFP (29) and GFP. An 8-μM GFP-*Tm*AFP solution in ammonium bicarbonate buffer was introduced into the microfluidic device and frozen by cooling the device to –20 °C. The temperature was gradually increased until a single ice crystal remained in one of the microchambers of the device (Fig. 2*B*). The temperature was then decreased to 0.05 °C below the melting point (still within the FH range) and kept constant throughout the experiment. The ice crystal was incubated in the GFP-*Tm*AFP solution for 20 min. Next, the main channel of the microfluidic device was slowly perfused with plain buffer, gradually removing unbound AFP molecules from the microchamber. After ~30 min of perfusion, fluorescence intensity of the solution surrounding the crystal became nearly undetectable (Fig. 2 *B* and *C*), indicating that only a small fraction (~2%) of the initial amount of GFP-*Tm*AFP remained in the microchamber (Fig. 2*C*, black line). In contrast, the fluorescence signal from the ice crystal surface was practically unchanged (Fig. 2*C*, green line), indicating that the GFP-*Tm*AFP molecules bound to the ice crystal remained adsorbed over the course of the medium exchange process. We estimated the density of the GFP-*Tm*AFP molecules on the ice surfaces from measurements of fluorescence intensity in the solution and at the ice surfaces, as described previously (22). We found surface densities ranging from 3,000 to 25,000 molecules per square micrometer, depending on the concentration in solution, plane of adsorption examined, and time allowed for accumulation. These surface densities correspond to distances between GFP-*Tm*AFP molecules ranging from 6 nm to 18 nm. These values of surface density are higher than those previously reported for AFGP and type III AFP (9, 22).

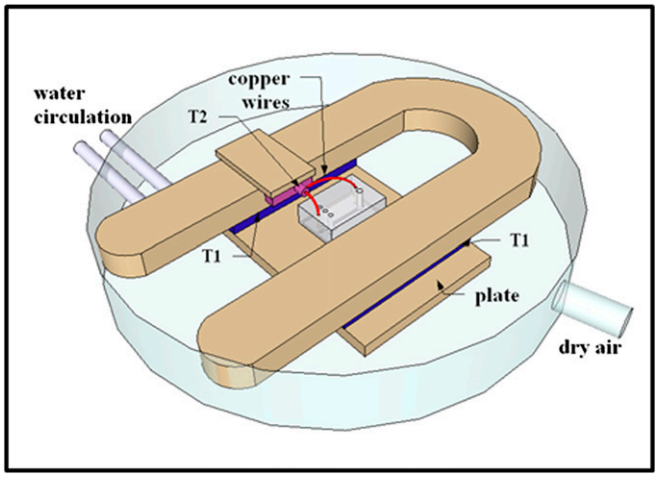

Fig. 1. Schematics of the experimental apparatus. The temperature in the microfluidic device is set using two temperature controllers connected to thermoelectric cooling elements (blue and purple), T1 from the bottom of the device through the copper plate and T2 from the top of the device through the copper wires (orange). A detailed description of the apparatus is provided in *SI Materials and Methods*.

In repeated experiments (n = 13), ice crystals grown in concentrated AFP solutions (5–40 μM) and then left in supercooled (by 0.05–0.10 °C) AFP-depleted solutions consistently showed no detectable growth for up to several hours (within our experimental resolution of ~1 μm). In contrast, ice crystals in water supercooled by 0.02 °C grew at a rate of ~4 μm/s. These results clearly demonstrated that AFP molecules bound to the ice surface did not readily desorb and return to the solution, and that these bound molecules were sufficient to prevent the ice crystals from growing.

Freezing Hysteresis Experiments in the Microfluidic Devices. To verify that the surface-bound AFPs remained active after the solution exchange and that the FH activity was not directly dependent on the AFP concentration in solution, a multistep experiment was performed (Fig. 3). As before, a GFP-*Tm*AFP solution was first frozen and slowly melted to obtain a single ice crystal in a microchamber (Fig. 3*A*). The ice crystal was incubated at a temperature 0.10 °C below the melting point for a period of 10 min. Following this stabilization period, the temperature was slowly decreased, while the size of the crystal was monitored. At a certain point, a sudden rapid growth of the crystal was observed (Fig. 3*B*), and the temperature at this point was defined as the nonequilibrium freezing temperature. The difference between the melting temperature and the nonequilibrium freezing temperature was called the freezing hysteresis activity before the AFP dilution, "FH-before". The frozen sample was then melted again until only a small ice crystal remained (Fig. 3*C*). The crystal was stabilized again for 10 min at a temperature 0.10 °C below the melting point. Following the stabilization period, the microfluidic device was perfused with plain buffer to gradually deplete GFP-*Tm*AFP molecules from the solution in the microchamber around the ice crystal (Fig. 3*D*, Fig. S1, and Movie S1). After GFP-*Tm*AFP was substantially depleted, a second FH measurement was conducted by gradually cooling the crystal until the nonequilibrium freezing point was reached, and the temperature difference between the melting and the new freezing point was called "FH-after". The FH-after and FH-before were close in value, with a ratio of 0.89 ± 0.08 (mean ± SEM; n = 8), even though the GFP-*Tm*AFP depletion reduced its concentration in solution by a factor >20 on average (Table S1 and Figs. S1 and S2). For example, in an experiment with an initial GFP-*Tm*AFP concentration of 13.3 μM and FH-before activity of 0.54 °C, after the solution was exchanged, its fluorescence intensity was reduced to 2% of its initial value, corresponding to 0.3 μM of GFP-*Tm*AFP. Nevertheless, the FH-after activity was measured as 0.50 °C, which was ~10 times greater than a typical value of FH activity of a 0.3-μM solution of GFP-*Tm*AFP (~0.05 °C). As a control, we performed experiments in which the solutions in the microchambers were frozen after the solution exchange and melted back to form new ice crystals from the AFP-depleted solution. The FH activity values of these crystals were just a few hundredths of a degree centigrade, matching the values for solutions with low concentrations of GFP-*Tm*AFP that we measured with a nanoliter osmometer. These findings indicate that the AFP molecules retained on a crystal surface during and after a major depletion of AFPs from solution are sufficient to protect the crystal to nearly the same extent as AFP molecules on the crystal surface at equilibrium with the initial, high-concentration AFP solution.

In yet another type of experiment, the same protocol as before was followed all of the way to the point of the FH-after measurement. The newly formed ice was then melted until an ice crystal slightly larger than the original crystal was obtained. Some of the outer regions of this new crystal were formed after the solution was exchanged and the AFP was greatly depleted, as indicated by substantially reduced fluorescence of these regions compared with an internal region of the crystal (which was a part of the original crystal). Therefore, the newly formed surface of this crystal was not expected to be as strongly protected by AFPs as the previous crystal. Indeed, the FH of this crystal was measured to be 0.02 °C,

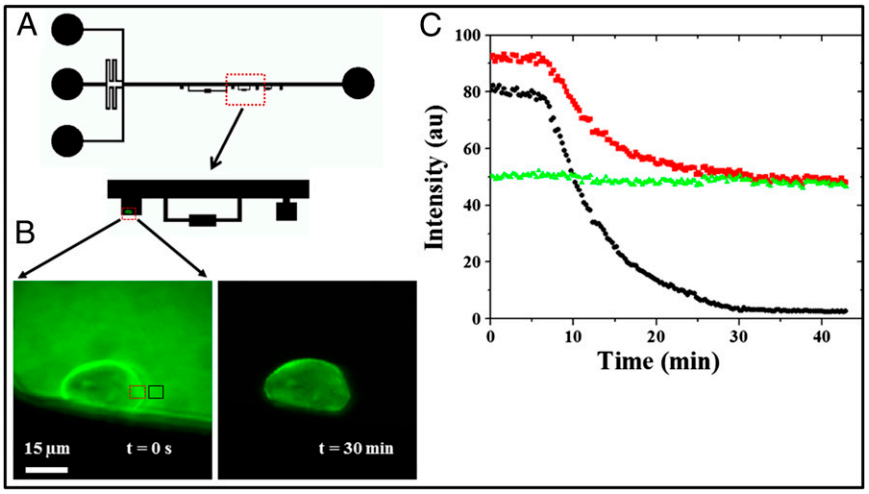

Fig. 2. Removal of free AFPs from the solution surrounding an AFP-coated ice crystal by solution exchange. (*A*) A schematic diagram of the microfluidic device and a magnified drawing of the area in the dashed-line box, showing a fragment of the main perfusion channel and three crystallization microchambers. (*B*) Fluorescence images of a microchamber with a single ice crystal grown in GFP-*Tm*AFP solution. The images were taken immediately before and during the solution exchange process. (*C*) Fluorescence intensity vs. time during the solution exchange for a region of the solution adjacent to the ice crystal (black box), for a region at the edge of the ice crystal (red box), and for the latter region excluding the contribution of fluorescence of GFP-*Tm*AFPs in solution (green). The last set of data points represents the fluorescence intensity of GFP-*Tm*AFPs adsorbed on the ice surface (Ice) and is calculated from the two first datasets, Solution and Edge, respectively, using the equation Ice = Edge − Const × Solution, where Const is a fitting parameter, which reflects the contribution of GFP-*Tm*AFPs in solution into the fluorescence at the edge of the ice crystal (22).

which was significantly lower than either the FH-before or the FH-after value (0.32 °C or 0.17 °C, respectively). As a next step, the temperature was increased to 0.002 °C above the melting temperature, and the ice crystal was melted until all newly formed regions with low fluorescence disappeared and the entire crystal surface was strongly fluorescent, indicating the presence of a dense layer of previously adsorbed AFPs. At this point, the crystal melting stopped, likely because of melting inhibition by the surface-adsorbed AFPs (30, 31). The FH of this third crystal was measured to be 0.25 °C, similar to the FH-before and FH-after values. The results of this experiment further corroborated that FH activity is provided by the surface-adsorbed AFPs and is not a direct function of concentration of AFPs in solution.

Time Dependence of FH Activity. The dependence of the FH activity on the time that was allowed for the adsorption of AFPs on an ice crystal was examined for GFP-*Tm*AFP with a custom-built nanoliter osmometer (32). We found that the FH activity increased with the time of exposure of the ice crystals to an AFP solution. Importantly, the activity improvement was significant even past the first 10 min of exposure, indicating that AFP adsorption to ice is a slow process (Fig. S3).

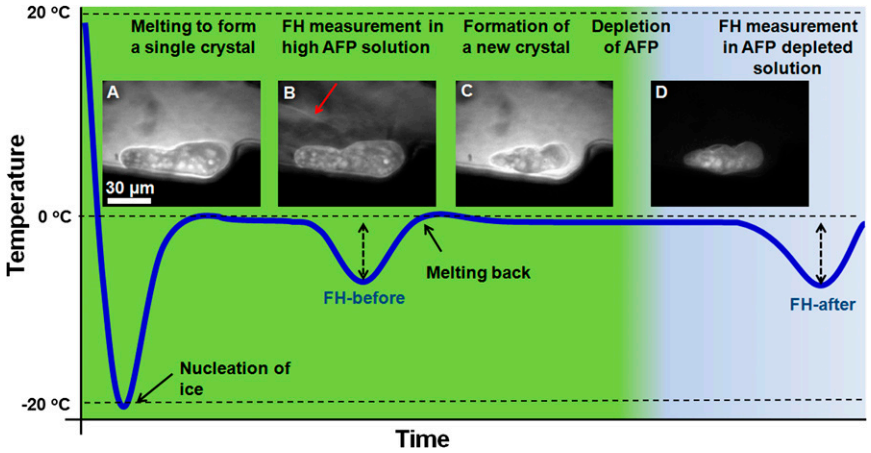

Fig. 3. Freezing hysteresis measurements in the microfluidic devices. Schematic plot shows the time course of changes in the temperature in crystallization chambers of the microfluidic device (note: the temperature changes are not to scale) juxtaposed with representative images of ice crystals at different stages of the experiment. (*A*) An AFP solution was frozen and melted back to form an ice crystal. The temperature was then slightly reduced (to stop the melting) and kept constant for ~10 min, with the ice crystal exposed to the AFP solution. (*B*) Next, the temperature was slowly reduced until the crystal started growing, and the ice freezing temperature was recorded. The difference between the melting temperature and this freezing temperature in the original AFP solution was defined as FH-before. (*C*) The ice was subsequently melted back, until a single small ice crystal remained. The temperature was again slightly reduced and kept constant for ~10 min. (*D*) The solution in the crystallization chamber was then exchanged with plain buffer, leading to nearly complete depletion of AFPs in solution around the crystal. Finally, the temperature was slowly reduced until the ice crystal started growing, and the new freezing temperature was used to calculate the value of FH-after, the FH activity after the depletion of AFPs.

Discussion

Several theoretical studies explained the experimentally observed concentration dependence of the FH activity by assuming that the adsorption of AFPs is reversible (11, 15–17). To investigate the binding kinetics at the ice–water interface and the dependence of FH on AFP concentration, it is important to understand the respective roles of AFPs in solution and AFPs bound to the ice surface. The use of microfluidics and the sensitive temperature-controlled system enabled slow removal of AFPs from the solution around individual small AFP-coated ice crystals without perturbing the temperature or exposing the crystals to any substantial hydrodynamic flow. The use of GFP-tagged AFPs and fluorescence microscopy made it possible to dynamically visualize and quantify the AFP depletion. In our experiments with hyperactive AFP from *T. molitor* fused with GFP, the fluorescence of ice crystals during and after the depletion of GFP-*Tm*AFP from the surrounding solution indicated a strong adsorption of AFPs to ice surfaces, to the point that it could be considered an irreversible binding. Importantly, the experiments clearly demonstrated that AFPs adsorbed on the surface of a supercooled ice crystal prevented it from growing even in the absence of AFPs in solution. It is evident from our experiments that once there is sufficient surface coverage of *Tm*AFP, FH activity is practically independent of concentration of AFPs in the solution. Our results do not support the theories that are based on the reversible-binding mechanism (9, 11, 15–17, 21, 33).

Knight and DeVries discussed the dynamic nature of concentration dependence of FH and stated that there is a competition between the rate of adsorption of AFPs to the ice surfaces and the rate of ice growth (19). Our experiments indicate that, at least for the *Tm*AFP, the FH is not a function of the concentration of AFPs in solution. Sander and Tkachenko developed the theory of kinetic pinning (20), which relates the concentration dependence of FH activity to the kinetics of crystal growth in line with Knight and DeVries' theory. According to their analysis, after the crystal growth is arrested, AFPs continue to accumulate on the surface until a saturation level is reached, which is imposed by steric limitations. The AFP accumulation would imply a gradual increase in FH over time, as was indeed observed in our experiments with hyperactive *Tm*AFP solutions (Fig. S3). The extended timescale (>10 min), at which the FH activity increased, indicates that the *Tm*AFP adsorption to ice is a relatively slow dynamic process. The existence of a slow adsorption and desorption rates was suggested recently by Kubota to explain the time-dependent behavior of the FH activity (34). The dynamic nature of the AFP adsorption was previously reported by other groups for two moderately active AFPs (35, 36). Thus, to ensure that the ice surface is well protected by AFPs, we exposed ice crystals to high concentrations of GFP-*Tm*AFP for at least 10 min before removing AFPs from the solution. Importantly, desorption of the AFP molecules in AFP-free solutions remained very small even at a timescale of 1 h (with both adsorption and desorption judged by the fluorescence intensity). Our results do not exclude AFP desorption on longer timescales (hours to days), and further experiments with crystals and solutions maintained at constant temperatures and monitored over extended periods of time are needed to examine this possibility.

A two-step binding model was proposed by Kristiansen and Zachariassen (33), in which they hypothesized an irreversible attachment of AFPs in the freezing hysteresis gap and the possibility of dynamic exchange of bound AFPs with free AFPs in solution at the equilibrium melting temperature, to explain the concentration dependence of FH. However, one could argue that the experimentally found melting hysteresis (30, 31) likely prevents a true equilibrium from forming. Additionally, the model does not take into account the possible accumulation of the proteins on the ice surface within the FH gap.

Ebbinghaus et al. argued that the activity of antifreeze glycoproteins is due to perturbation of the solution over long distances and thus the adsorption to ice surfaces through direct bonding is not necessarily the molecular mechanism for the antifreeze activity (37). In contrast, our experiments strongly indicate that surface-adsorbed AFPs are the core source of crystal protection against freezing. The correlation between the presence of AFP molecules and modifications of water dynamics at the far hydration shells may be a consequence of the ability of AFPs to order water molecules on their surface (38). This ability makes AFPs compatible with the ice surface structure, allowing them to stabilize the ice–water interface (39), and this stabilization results in freezing hysteresis. A recent work has shown that the ice-binding face of an AFP can hold water molecules in an organized array resembling the molecular structure of ice surfaces (40). According to this anchored clathrate water hypothesis, the ice-binding site of the AFP forms its ligand (an ice-like lattice of water molecules) before merging with the ice. These AFP-bound water molecules can promote stable adhesion of AFPs to the ice surfaces. Our results are in agreement with the latter hypothesis, as well as with other studies that suggest direct binding of AFP to ice crystals.

In summary, the present study used fluorescence microscopy, a specially designed microfluidic device, and a precise temperature-controlled experimental setup to investigate the interaction of AFPs with ice crystals. We performed and recorded a gradual removal of GFP-tagged *Tm*AFP molecules from solution around unperturbed ice crystals. Whereas AFP in solution was greatly depleted, the amount of AFP molecules adsorbed on the crystal surface remained nearly unchanged, indicating practically irreversible binding of *Tm*AFPs to the ice. Furthermore, the experiments showed that the presence of AFP molecules on the ice surface leads to substantial FH activity, even if there are virtually no AFP molecules in solution. Whereas antifreeze protein molecules in solution may have physical effects of their own, the presented results suggest that these effects are not directly related to the ice growth inhibition activity of the antifreeze protein that was examined. The findings of this work advance the general understanding of the mechanism of action of AFPs, and the presented experimental setup can be a powerful tool for investigation of AFPs and their function at precisely controlled subzero temperatures.

Materials and Methods

Protein Sample Preparation. The recombinant fusion protein, consisting of GFP linked to *Tm*AFP, was expressed and purified in the laboratory of Deborah Fass (Weizmann Institute of Science, Rehovot, Israel), as described previously (41). Aliquots of GFP-*Tm*AFP were stored in a 20-mM ammonium bicarbonate buffer (pH 8) at −20 °C.

Microfluidic Apparatus. The microfluidic devices were fabricated by soft lithography and replica-molding techniques from polydimethylsiloxane (PDMS) (42). The molds were prepared using photolithography of a UV-curable epoxy (SU8 2010; Microchem), following the manufacturer's instructions to create a 15- to 20-μm tall relief. PDMS chips were bonded to glass coverslips, using treatment in an oxygen plasma cleaner (Harrick Plasma Cleaner; model PDC-32G). Each microfluidic device has two inlets, an outlet, and a vent. The microchannel array of the device includes the main perfusion channel and several crystallization microchambers on its sides with different shapes and sizes ranging from 100 to 200 μm. The microfluidic device was mounted on a copper plate with a 0.75-mm–wide slit opening, designed for visualization of the ice crystals in the microchambers using an inverted fluorescence microscope. The small width of the slit and the high thermal conductivity of copper minimized temperature gradients in the device. Thermal contact between the microfluidic device and the copper plate was enhanced by a thin layer of oil. In some of the experiments, a sapphire coverslip was placed between the glass coverslip and the copper plate, further reducing the temperature gradient due to much higher thermal conductivity of sapphire compared with glass. The device was placed into a temperature-controlled cell that included two thermoelectric Peltier cooling elements, a thermistor, and a temperature controller (model 3040 or 3150; Newport). A continuous slow flow of dry air through the cell was used to minimize the condensation

of water on the cold parts inside it. This custom-designed temperature-controlled system enabled setting the temperature of the copper plate as low as –25.0 °C with a 0.001 °C resolution. An additional temperature control circuit that included a heater and copper wires embedded in the PDMS microfluidic device adjacent to the inlets and outlet was used to locally melt the peripheral ice.

Temperature Profile in Microfluidic Devices. The distribution of temperature in the microfluidic device was examined using 3D simulations in Comsol Multiphysics software. The simulations incorporated the dimensions and thermal conductivities of the copper plate, coverslip, and PDMS microfluidic device (further details in *SI Materials and Methods*). Because of relatively low thermal conductivities of glass and PDMS and low temperature of the copper plate (>20 °C below the room temperature), there was an ∼0.06 °C variation of temperature across the slit that translated into a temperature gradient of 0.01 °C/100 μm across the crystallization microchambers. For an ice crystal with a typical size of 30 μm, the temperature nonuniformity was expected to be less than 0.01 °C, with only minor effects on the experimental results. The numerical simulations also indicated that the use of a sapphire coverslip practically eliminated the temperature gradient in the microchambers, reducing it to 0.001 °C/100 μm (Fig. S4), corresponding to <0.001 °C temperature variation across an ice crystal. The sapphire coverslip (which was used only in a part of the reported experiments) allowed obtaining stable crystals in the middle of the microchambers rather than near their edges. Most importantly, as indicated by the dynamics of the ice front in the microchambers in response to changes in the temperature controller settings, the system provided ∼0.002 °C precision and stability in the control of temperature in a given area of a microchamber (Fig. S5, Movie S2, and *SI Materials and Methods*).

Protocol to Form a Single Ice Crystal Within a Microfluidic Chamber. The flow through the microfluidic device was driven and controlled by hydrostatically generated differential pressure between the device's inlets and outlet. The two inlets of the device were connected to two reservoirs with a buffer solution through thin lines of tubing. One of the tubing lines had a connector allowing the injection of a small amount (∼3 μL) of protein solution into a short segment of the line, serving as a miniature reservoir just upstream of the device inlet. This method minimized the consumption of proteins in the experiment. The medium in the microchambers was exchanged by changing the inlet pressures, thus alternatively feeding solutions with and without protein into the main channel of the device, as described in ref. 43. For long incubation, the inlets were externally blocked. To form isolated ice crystals in the device microchambers, the copper plate temperature was first set at approximately –20 °C, thereby freezing liquid in the entire device. Next, the stage was warmed to ∼0.02 °C below the melting temperature. At this point, the copper wires near the device inlets and outlet were warmed to free them from ice. Therefore, the only ice remaining was contained within the microchannels in the microfluidic device. The temperature of the copper plate was then carefully increased, until only a small ice crystal (20–50 μm) remained in one of the microchambers. From this point on, copper wires were not heated. To exchange the solution around the crystal, plain buffer was perfused through the main channel of the device, causing gradual elution of AFPs from the microchamber with the crystal. We empirically found that at flow rates in a 0.4- to 0.6-μL/min range, corresponding to a flow velocity in the range of 2–3 mm/s in the main channel, ice crystals remained stable for extended time intervals, whereas higher flow rates, in a range of 6–10 μL/min, resulted in occasional melting of the crystals. The melting might have been caused by a perturbation of the immediate vicinity of the crystals by the flow or by relatively high temperature of the perfusion liquid, which was not allowed enough time to equilibrate with the cold copper plate. Even when ice crystals survived the high perfusion rates, a reduction in the measured FH-after was observed. Therefore, only the data obtained with perfusion rates of 0.4–0.6 μL/min were included in our analysis.

Visualizing Surface-Bound GFP-*Tm*AFPs on Ice Crystals. An inverted fluorescence microscope (Nikon TE2000-U; Nikon Instruments) was used to image the samples. The imaging was performed with two long working-distance (WD) Nikon objectives: 50×, NA 0.55, WD 8.7 mm and 10×, NA 0.25, WD 10.1 mm. The images were analyzed using WinView32 imaging software (Roper Scientific). Samples were illuminated by a 488-nm beam derived from an Argon laser. The fluorescence signal from an ice crystal surface was treated as a sum of fluorescence of GFP-*Tm*AFP molecules bound to the crystal in the part of the optical detection volume occupied by the crystal and free GFP-*Tm*AFP molecules in the solution part of the detection volume (22). The latter contribution was appreciable because of relatively large dimensions of the detection volume (and wide-field rather than confocal imaging) and was considered to be proportional to the fluorescence intensity of the solution away from the crystal. We measured the dependences of fluorescence of different regions of the crystal surface on the fluorescence of solution away from the crystal during the depletion of GFP-*Tm*AFP from the microchamber (Fig. 2*C*). The dependences could be fitted with a linear relation with a single free parameter (the relative contribution of the solution into the fluorescence signal). The fluorescence of the crystal surface calculated using this procedure was nearly independent of the fluorescence of the solution, strongly indicating that the amount of GFP-*Tm*AFP bound to the ice crystal was not affected by depletion of free GFP-*Tm*AFP from the solution. A similar approach was used previously by Pertaya et al. (22). This finding was further supported by the observed constant fluorescence intensity at the crystal surface after the exchange of the GFP-*Tm*AFP solution with plain buffer was practically complete, as shown in the last ∼10 min of dependence in Fig. 2*C*.

Nanoliter Osmometer Experiments to Investigate the Time Dependence of FH. We performed nanoliter osmometer experiments in which we varied the exposure time of ice crystals to the AFP solutions before measuring the FH activity, as explained in detail in *SI Materials and Methods*.

ACKNOWLEDGMENTS. The authors thank Liwei Chen, Savas Kaya, Yunxiang Gao, Kyle Campbell, and Yangzhong Qin for their help during the microfluidic device fabrication process and Avigail Ben-Or for assistance with data analysis. This work was supported by the National Science Foundation, a Marie Curie reintegration grant, the Israel Science Foundation, the European Research Council, the Canadian Institutes of Health Research, the Condensed Matter and Surface Science program at Ohio University, and the Otto Warburg Minerva Center for Agricultural Biotechnology.

1. DeVries AL, Komatsu SK, Feeney RE (1970) Chemical and physical properties of freezing point-depressing glycoproteins from Antarctic fishes. *J Biol Chem* 245(11): 2901–2908.
2. Duman JG (2001) Antifreeze and ice nucleator proteins in terrestrial arthropods. *Annu Rev Physiol* 63:327–357.
3. Middleton AJ, et al. (2012) Antifreeze protein from freeze-tolerant grass has a beta-roll fold with an irregularly structured ice-binding site. *J Mol Biol* 416(5):713–724.
4. Janech MG, Krell A, Mock T, Kang JS, Raymond JA (2006) Ice-binding proteins from sea ice diatoms (Bacillariophyceae). *J Phycol* 42(2):410–416.
5. Scotter AJ, et al. (2006) The basis for hyperactivity of antifreeze proteins. *Cryobiology* 53(2):229–239.
6. Knight CA, Cheng CC, DeVries AL (1991) Adsorption of alpha-helical antifreeze peptides on specific ice crystal surface planes. *Biophys J* 59(2):409–418.
7. Raymond JA, DeVries AL (1977) Adsorption inhibition as a mechanism of freezing resistance in polar fishes. *Proc Natl Acad Sci USA* 74(6):2589–2593.
8. Knight CA, Wierzbicki A (2001) Adsorption of biomolecules to ice and their effects upon ice growth. 2. A discussion of the basic mechanism of "antifreeze" phenomena. *Cryst Growth Des* 1(6):439–446.
9. Zepeda S, Yokoyama E, Uda Y, Katagiri C, Furukawa Y (2008) In situ observation of antifreeze glycoprotein kinetics at the ice interface reveals a two-step reversible adsorption mechanism. *Cryst Growth Des* 8(10):3666–3672.
10. Wierzbicki A, et al. (2007) Antifreeze proteins at the ice/water interface: Three calculated discriminating properties for orientation of type I proteins. *Biophys J* 93(5): 1442–1451.
11. Burcham TS, Osuga DT, Yeh Y, Feeney RE (1986) A kinetic description of antifreeze glycoprotein activity. *J Biol Chem* 261(14):6390–6397.
12. Beaglehole D, Wilson P (1993) Thickness and anisotropy of the ice water interface. *J Phys Chem* 97(42):11053–11055.
13. Hew CL, Yang DSC (1992) Protein interaction with ice. *Eur J Biochem* 203(1–2):33–42.
14. Hall DG, Lips A (1999) Phenomenology and mechanism of antifreeze peptide activity. *Langmuir* 15(6):1905–1912.
15. Jorov A, Zhorov BS, Yang DS (2004) Theoretical study of interaction of winter flounder antifreeze protein with ice. *Protein Sci* 13(6):1524–1537.
16. Li QZ, Yeh Y, Liu JJ, Feeney RE, Krishnan VV (2006) A two-dimensional adsorption kinetic model for thermal hysteresis activity in antifreeze proteins. *J Chem Phys* 124 (20):204702.
17. Liu JJ, Li QZ (2006) Theoretical model of antifreeze protein-ice adsorption: Binding of large ligands to a two-dimensional homogeneous lattice. *Chem Phys Lett* 422(1–3): 67–71.
18. Wang S, Amornwittawat N, Wen X (2012) Thermodynamic analysis of thermal hysteresis: Mechanistic insights into biological antifreezes. *J Chem Thermodyn* 53: 125–130.
19. Knight CA, DeVries AL (2009) Ice growth in supercooled solutions of a biological "antifreeze", AFGP 1-5: An explanation in terms of adsorption rate for the concentration dependence of the freezing point. *Phys Chem Chem Phys* 11(27):5749–5761.
20. Sander LM, Tkachenko AV (2004) Kinetic pinning and biological antifreezes. *Phys Rev Lett* 93(12):128102.

21. Ba Y, Wongskhaluang J, Li J (2003) Reversible binding of the HPLC6 isoform of type I antifreeze proteins to ice surfaces and the antifreeze mechanism studied by multiple quantum filtering-spin exchange NMR experiment. *J Am Chem Soc* 125(2):330–331.
22. Pertaya N, et al. (2007) Fluorescence microscopy evidence for quasi-permanent attachment of antifreeze proteins to ice surfaces. *Biophys J* 92(10):3663–3673.
23. Sönnichsen FD, Sykes BD, Chao H, Davies PL (1993) The nonhelical structure of antifreeze protein type III. *Science* 259(5098):1154–1157.
24. Stan CA, et al. (2009) A microfluidic apparatus for the study of ice nucleation in supercooled water drops. *Lab Chip* 9(16):2293–2305.
25. Edd JF, Humphry KJ, Irimia D, Weitz DA, Toner M (2009) Nucleation and solidification in static arrays of monodisperse drops. *Lab Chip* 9(13):1859–1865.
26. Sgro AE, Chiu DT (2010) Droplet freezing, docking, and the exchange of immiscible phase and surfactant around frozen droplets. *Lab Chip* 10(14):1873–1877.
27. Kintses B, van Vliet LD, Devenish SR, Hollfelder F (2010) Microfluidic droplets: New integrated workflows for biological experiments. *Curr Opin Chem Biol* 14(5):548–555.
28. Gui L, Yu BY, Ren CL, Huissoon JP (2011) Microfluidic phase change valve with a two-level cooling/heating system. *Microfluid Nanofluid* 10(2):435–445.
29. Liou YC, Tocilj A, Davies PL, Jia ZC (2000) Mimicry of ice structure by surface hydroxyls and water of a beta-helix antifreeze protein. *Nature* 406(6793):322–324.
30. Celik Y, et al. (2010) Superheating of ice crystals in antifreeze protein solutions. *Proc Natl Acad Sci USA* 107(12):5423–5428.
31. Knight CA, Devries AL (1989) Melting inhibition and superheating of ice by an antifreeze glycopeptide. *Science* 245(4917):505–507.
32. Bar M, Celik Y, Fass D, Braslavsky I (2008) Interactions of beta-helical antifreeze protein mutants with ice. *Cryst Growth Des* 8(8):2954–2963.
33. Kristiansen E, Zachariassen KE (2005) The mechanism by which fish antifreeze proteins cause thermal hysteresis. *Cryobiology* 51(3):262–280.
34. Kubota N (2011) Effects of cooling rate, annealing time and biological antifreeze concentration on thermal hysteresis reading. *Cryobiology* 63(3):198–209.
35. Chapsky L, Rubinsky B (1997) Kinetics of antifreeze protein-induced ice growth inhibition. *FEBS Lett* 412(1):241–244.
36. Takamichi M, Nishimiya Y, Miura A, Tsuda S (2007) Effect of annealing time of an ice crystal on the activity of type III antifreeze protein. *FEBS J* 274(24):6469–6476.
37. Ebbinghaus S, et al. (2010) Antifreeze glycoprotein activity correlates with long-range protein-water dynamics. *J Am Chem Soc* 132(35):12210–12211.
38. Nutt DR, Smith JC (2008) Dual function of the hydration layer around an antifreeze protein revealed by atomistic molecular dynamics simulations. *J Am Chem Soc* 130 (39):13066–13073.
39. Wierzbicki A, Madura JD, Salmon C, Sönnichsen F (1997) Modeling studies of binding of sea raven type II antifreeze protein to ice. *J Chem Inf Comput Sci* 37(6):1006–1010.
40. Garnham CP, Campbell RL, Davies PL (2011) Anchored clathrate waters bind antifreeze proteins to ice. *Proc Natl Acad Sci USA* 108(18):7363–7367.
41. Bar M, Bar-Ziv R, Scherf T, Fass D (2006) Efficient production of a folded and functional, highly disulfide-bonded beta-helix antifreeze protein in bacteria. *Protein Expr Purif* 48(2):243–252.
42. Zaouk R, Park BY, Madou MJ (2006) in *Microfluidic Techniques*, ed Minteer SD (Humana Press, Totowa, NJ), pp 17–21.
43. Groisman A, et al. (2005) A microfluidic chemostat for experiments with bacterial and yeast cells. *Nat Methods* 2(9):685–689.